Preferential Heating and Acceleration of α Particles by Alfvén-Cyclotron Waves

J. A. Araneda*
Departamento de Física, Universidad de Concepción, Concepción 4070386, Chile
Y. Maneva† and E. Marsch‡
Max-Planck Institut für Sonnensystemforschung, Katlenburg-Lindau 37191, Germany
(Received 22 October 2008; published 27 April 2009)

Preferential heating and acceleration of heavy ions in the solar wind and corona represent a long-standing theoretical problem in space physics, and are distinct experimental signatures of kinetic processes occurring in collisionless plasmas. We show that fast and slow ion-acoustic waves (IAW) and transverse waves, driven by Alfvén-cyclotron wave parametric instabilities can selectively destroy the coherent fluid motion of different ion species and, in this way lead to their differential heating and acceleration. Trapping of the more abundant protons by the fast IAW generates a proton beam with drift speed of about the Alfvén speed. Because of their larger mass, α particles do not become significantly trapped and start, by conservation of total ion momentum, drifting relative to the receding bulk protons. Thus the resulting core protons and the α particles are differentially heated via pitch-angle scattering.

DOI: 10.1103/PhysRevLett.102.175001 PACS numbers: 52.35.Mw, 94.05.−a, 96.50.Ci

In situ measurements in the solar wind [1] and remote-sensing observations of the solar corona [2] have clearly shown that the heavy minor ions in these essentially collisionless space plasmas are heated and accelerated preferentially as compared to the major protons and electrons. The identification and explanation of the physical mechanisms responsible for this may provide a key to explaining why the temperature of the outer solar atmosphere and expanding corona forming the solar wind is by 2 to 3 orders of magnitude higher than that of the photosphere, i.e., the visible solar surface. Maintaining such a high temperature requires an efficient dissipation process converting coherent mechanical or electromagnetic energy into random thermal particle energy.

Any coronal heating model must be able to describe the ample solar observations [2–5] made in coronal holes by UVCS (ultraviolet coronagraph spectrometer) and SUMER (solar ultraviolet measurements of emitted radiation) on the SOHO (solar and heliospheric observatory) spacecraft, which show from line broadenings that heavy ions are much hotter than protons, and that the velocity distribution function (VDF) of the oxygen ion O^{5+} appears to be strongly anisotropic, with $T_{\perp i}/T_{\|i} \gg 1$ (here $\perp$ and $\|$ denote orthogonal perpendicular and parallel directions relative to the background magnetic field $\mathbf{B}_0$). These remote-sensing observations impose severe constrains on the coronal ion heating mechanism.

The extreme departures from thermodynamic equilibrium found in coronal holes are qualitatively consistent with the *in situ* plasma measurements. Namely, ion VDFs in high-speed solar wind streams exhibit characteristic nonthermal features [1], which are often associated with large-amplitude Alfvénic fluctuations [6–8], enhanced activity of ion-acoustic waves (IAW) [9], and electric field fluctuations in the ion-cyclotron frequency range [10,11]. Proton VDFs typically show a denser proton core component, having a temperature anisotropy with $T_{\perp \mathrm{pc}}/T_{\|\mathrm{pc}} \approx 2$, and a more dilute beamlike or secondary component streaming away from the Sun along $\mathbf{B}_0$ at about 1.5 the local Alfvén speed V_A [12–14]. Alpha particles (He_4^{2+}) and other heavier ions are also observed to stream faster than the protons by a sizable fraction of the local Alfvén speed, and to be hotter in mass proportion, with $T_i \gtrsim (m_i/m_p)T_p$ [1,15,16].

In a recent analytical and hybrid-simulation study on parametric instabilities of Alfvén-cyclotron waves [17], ion trapping in the nonlinear driven IAW and pitch-angle scattering in the transverse daughter waves were found to be responsible for the anisotropic core heating and beam formation of proton VDFs, in close agreement with the observed kinetic features in the solar wind [1]. Later on, low-noise Vlasov-Maxwell simulations of left-hand polarized Alfvén-cyclotron waves [18] showed that, simultaneously with the increase of $T_{\perp p}$, bursts of ion-acoustic activity are produced together with particle trapping and beam formation. The simulated IAW spectra were shown to be consistent with the electrostatic waves actually measured in the solar wind [9], and the results interpreted as providing links between the macroscopic and microscopic scales in solar-wind turbulence.

In this Letter, we will corroborate the preferential heating and acceleration mechanism by parametrically unstable Alfvén-cyclotron waves in a multi-ion-species plasma. The theory and simulations presented below reproduce, for the first time to our knowledge, the main nonthermal features of the VDFs of protons and α particles as measured in the fast solar wind.

An important and basic fact exploited here is that a circularly polarized Alfvén wave not only is a solution of the MHD equations, but also is an exact nonlinear solution of the full Vlasov-Maxwell equations, even if the plasma contains several particle species [19]. Actually, the recent images obtained with high temporal and spatial resolution by the Solar Optical Telescope (SOT) onboard the Hinode satellite have revealed that the chromosphere, the interface between the solar photosphere and the lower corona, is permeated by strong Alfvén waves [20]. By estimating their energy density and comparing it with results from MHD simulations, it was found that those Alfvén waves have enough energy to accelerate the solar wind and to heat the corona. Such fluctuations at large MHD scales may drive both a parallel and a perpendicular nonlinear energy cascade towards the kinetic regime [21,22]. In fact, an exhaustive data analysis of solar-wind proton and α-particle temperatures has shown clear evidence of Alfvén-cyclotron dissipation, with the relative absorption rates being regulated by the drift speed between the two species [23]. Therefore, studying basic nonlinear processes of such waves at kinetic scales will give us new insights into the ion heating problem and particle acceleration in astrophysical plasmas [21–25].

The simulations have been carried out with an electromagnetic hybrid code [17], where the ions are treated kinetically while the electrons are considered as an isothermal massless fluid. The code is 1D in space but retains the three components of the particle velocities and electromagnetic fields. The plasma is magnetized, quasineutral, and consists of protons and a small population of α particles. All computations are performed in the ion center-of-mass frame. At $t = 0$, the plasma has uniform density, and a circularly left-hand polarized parent wave train is propagating along $\mathbf{B}_0 = B_0\hat{\mathbf{z}}$. The wave, with amplitude δB, wave number k_0, and frequency ω_0 is given by the expression

$$\delta\mathbf{B} = \delta B[\cos(k_0 z - \omega_0 t)\hat{\mathbf{x}} + \sin(k_0 z - \omega_0 t)\hat{\mathbf{y}}]. \quad (1)$$

The self-consistent initial ion VDFs are isotropic and spatially uniform nondrifting Maxwellians with a transverse bulk velocity [19]

$$\mathbf{V}_{\perp i} = -\frac{(\omega_0/k_0)}{1 - \omega_0/\Omega_i}\delta\mathbf{B}, \quad (2)$$

reflecting the ion sloshing in the wave. Here Ω_i is the ion-cyclotron frequency based on the background magnetic field. The system of length $2\pi m_0/k_0$ ($m_0 = 32$) has periodic boundary conditions, 2048 cells, and contains per cell 800 particles of each ion species. The normalized time step is $dt\Omega_p^{-1} = 0.03$, and the positions are normalized to the proton skin depth, $V_A\Omega_p^{-1}$, with $V_A = B_0/(\mu_0 n_e m_p)^{1/2}$ being the Alfvén speed. The parent wave has a relative amplitude $\delta B/B_0 = 0.25$, $k_0 = 0.4\Omega_p/V_A$, $\omega_0 = 0.301\Omega_p$, and satisfies the exact (i.e., without any perturbation analysis) dispersion relation [19]

$$k_0^2 - \frac{\omega_0^2}{c^2} + \frac{1}{c^2}\sum_s \omega_{\mathrm{ps}}^2 \frac{\omega_0}{\omega_0 - \Omega_s} = 0. \quad (3)$$

For frequencies well below $|\Omega_e|$, Eq. (3) takes the form

$$k_0^2 - \frac{\mu_0}{B_0^2}\sum_{i\neq e} \frac{n_i m_i \omega_0^2}{1 - \omega_0/\Omega_i} = 0. \quad (4)$$

Therefore, using Eqs. (1), (2), and (4) we can prepare the multispecies plasma in an analytically exact initial state. However, due to the finite temperature of the plasma, coupling of the parent wave to smaller-amplitude spontaneous fluctuations generates parametric instabilities, a process by means of which the energy of the fluid motion and in the wave is gradually transferred to incoherent kinetic ion motion. In order to demonstrate the resulting differential ion heating, we chose plasma parameters with relative low plasma beta, $\beta_{\|j} = 2\mu_0 n_j k_B T_{\|j}/B_0^2$, where the parallel ion temperature is related to the thermal speed by $v_j = \sqrt{2k_B T_{\|j}/m_j}$. Thus, $\beta_{\|\alpha} = 3.63 \times 10^{-3}$, $\beta_{\|\alpha}/\beta_{\|p} = 0.1$, and $n_\alpha/n_p = 0.05$, corresponding to typical conditions in fast solar wind close to the corona. Because of the large number of free adjustable parameters, we use kinetic theory [26] to guide their choice for our simulations and to identify the possible instabilities.

During the linear stage two types of instabilities emerge: a modulational (M) and a decaylike (D) instability. In accord with kinetic theory [26], the IAW driven by the M instability have a relative constant and high phase speed, with $\omega_r/k \sim 0.65V_A$, which therefore we name fast IAW. The slow mode corresponds to IAW driven by the D instability, with decreasing but positive phase speed, and $\omega_r/k \sim 0.15V_A$ at the maximum growth rate. For dispersive Alfvén waves both instabilities are generally present and, depending on the values of β_i, one or the other can be dominant. Thus, ions moving close to the phase velocity of these driven IAW will be in resonance and thus may extract significant wave energy. Note that due to the low-β_i values and low ω_0, cyclotron resonance is unlikely [17,27,28].

Figure 1 shows phase space diagrams of the ion VDFs at the times $\Omega_p t \approx 486$ and 642. When comparing the phase plots of both ion components, we can observe that a large number of protons have been trapped and follow closed orbits around the phase speed of the fast IAW mode, whereby particles on the tail of the proton VDF are reaching up to twice the phase speed. In contrast, the heavier α particles perform a sloshing motion along $\mathbf{B}_0$ and do not exhibit significant trapping. It is worth mentioning that fast and slow IAW have also been observed in the two-ion-species plasmas of laser-fusion experiments, where evidence for hot ions created by trapping was found [29]. Thompson scattering measurements of the growth of IAW in a beryllium plasma (doped with a small fraction of gold) revealed that only the Be-like fast IAW mode grows and heats the ions.

Figure 2 displays contour plots of the ion VDFs in the (v_x, v_z) plane at the times $\Omega_p t \approx 16$, 564, and 2005. The

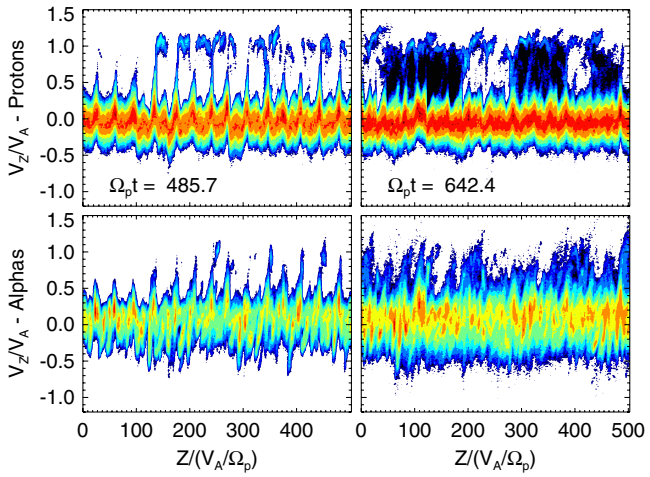

FIG. 1 (color online). Top: $v_z - z$ proton phase space at $\Omega_p t = 485.7$, and $\Omega_p t = 642.4$, respectively. Bottom: α-particle phase space at the same instants of time.

left panel shows the time evolution of the proton VDF revealing the gradual appearance of a field-aligned tail or proton beam at speed $v_z \gtrsim V_A$. Simultaneously with the trapping process by the IAW, a parabolic shell-like reshaping of the core at negative velocities takes place, and partial filling of the plateau between core and beam occurs. These processes are due to the destruction of the coherent fluid-like motion of the particles by the parallel electric field fluctuations associated with the slow and fast IAW. They change the parallel velocity of the ions inducing a pitch-angle scattering by the decreasing parent wave, but also by the growing forward-propagating sideband transverse waves driven by the M instability, and by the backward transverse waves (which are due to the D instability). Such mechanisms give the VDF its distinctive anisotropically heated core, in agreement with previous works and observations [17,18,30,31].

The right panel shows the corresponding time evolution of the VDF of the α particles. Their apparent initial anisotropy is due to the overlapping of the particle transverse paths of motion as imposed by the pump wave. Since they are cool, heavier, and their density much lower, the number of resonant particles on the tail is too small for trapping by the fast IAW. The slow IAW induce only a sloshing ion motion in the bulk of the distributions along $\mathbf{B}_0$. The transverse waves contribute mainly to the heating, but only indirectly (through the couplings) to a net acceleration of the particles. The α particles fill a larger part of velocity space because they have a lower gyrofrequency, and also because they have initially a larger transverse bulk velocity (due again to their lower gyrofrequency). Thus, the differential motion between the two different species occurs due to the proton beam formation and total ion momentum conservation along the magnetic field. Such morphological features of the VDFs have in fact been observed by *in situ* measurements made with the 3D plasma experiments onboard the Helios and PHOBOS II spacecrafts [12,32,33].

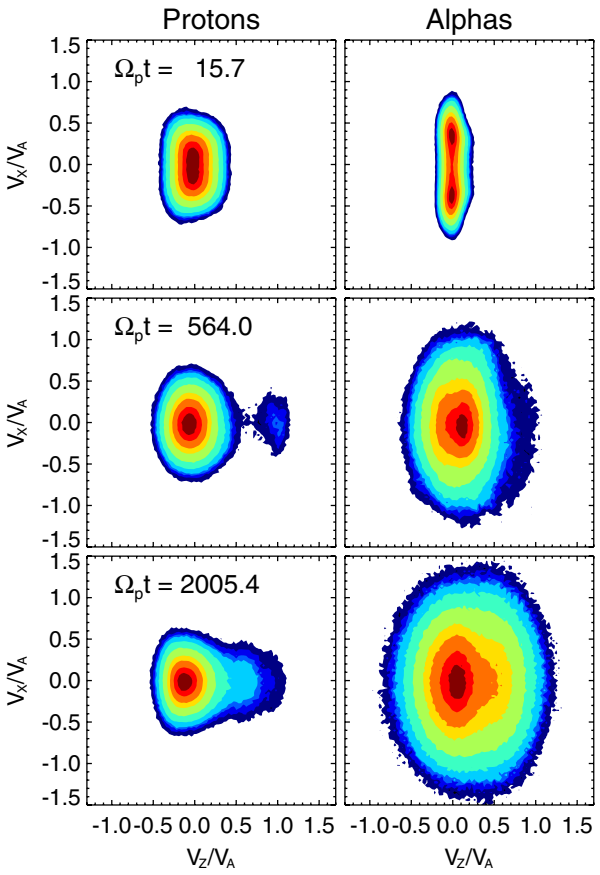

FIG. 2 (color online). Left: Contour plots of the proton VDFs in the (v_x, v_z) plane at three instants of time. Right: contour plots of the α-particle VDF at the same times. The proton beam reaches a relative number density of about 6%.

Figure 3 shows the evolution of $T_\parallel$ and $T_\perp$ of protons and α particles as functions of time. The apparent abrupt increase of $T_{\perp\alpha}$ at the beginning of the simulation is due only to the imposed transverse fluid motion by the parent wave, and thus it does not correspond to real heating.

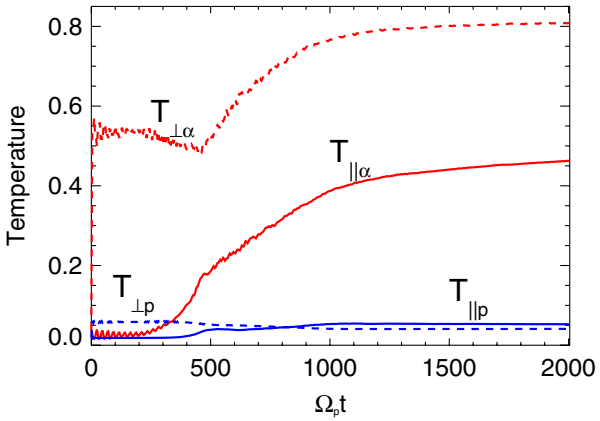

FIG. 3 (color online). Time history of the parallel (solid lines) and perpendicular (dashed lines) temperatures of protons and α particles.

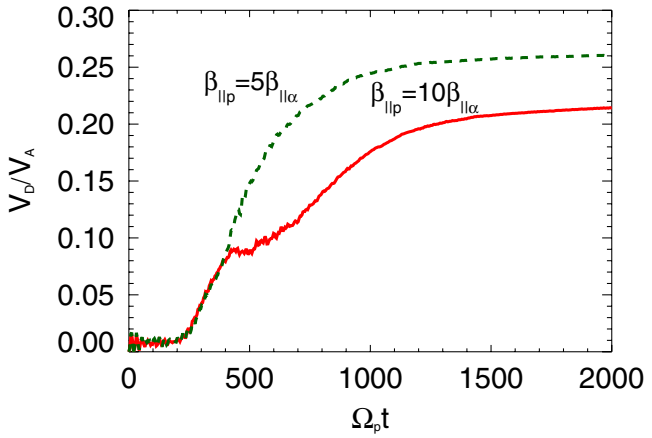

FIG. 4 (color online). Time history of the relative drift speed in units of Alfvén speed between α particles and protons. Solid line for the same parameters as in Figs. 1–3. The dashed line represents the case with $\beta_{\|\alpha}/\beta_{\|p} = 0.2$, while the other parameters are unchanged.

However, after the saturation period (around $t = 500\Omega_p^{-1}$), effective heating occurs due to the transfer of the initial fluid-motion energy to particle random motion by means of the scattering mechanisms mentioned above, as is evident in the VDFs plots of Fig. 2. Note also that the overall proton thermal anisotropy is $T_{p\perp}/T_{p\|} \lesssim 1$ at the end of the simulation run, but the proton core VDF still has $T_{\mathrm{pc}\perp}/T_{\mathrm{pc}\|} \gtrsim 1$ in Fig. 2, in good agreement with observed features [1,23].

Figure 4 displays the time history of the relative drift speed between α particles and protons, V_D. It reveals that the differential motion takes place simultaneously with the proton trapping and beam formation. The speed difference reaches a saturation value of about $\sim 0.2 V_A$ at the end of the simulation (solid line). We repeated the simulation using the same parameters as above, except that $\beta_{\|\alpha}/\beta_{\|p} = 0.2$, corresponding to the case where the protons are by 50% colder, but the thermal speed is the same for both ion species. The result is that V_D reaches a larger value, confirming again the supposition that kinetic effects are important even for low-β plasmas. With a slight reduction of the α density, for example, to $n_\alpha/n_p = 0.03$, the final relative drift turns out to be even larger. For large β_i values the number of particles on the tails increases and the larger inertia of the resulting beam hinders the system to reach large drift speeds. Consequently, kinetic processes may already take place in the early expansion of the fast solar wind near the Sun [1], and also cause the break found in the slope of observed turbulence spectra at scales near the proton inertial length, likely in relation to fluctuations in the ion-cyclotron-frequency range.

*jaraneda@udec.cl
†maneva@linmpi.mpg.de
‡marsch@linmpi.mpg.de

[1] E. Marsch, Living Rev. Solar Phys. **3**, 1 (2006).
[2] J. L. Kohl *et al.*, Astron. Astrophys. Rev. **13**, 31 (2006).
[3] S. R. Cranmer *et al.*, Astrophys. J. **678**, 1480 (2008).
[4] L. Dolla and J. Solomon, Astron. Astrophys. **483**, 271 (2008).
[5] K. Wilhelm *et al.*, Space Sci. Rev. **133**, 103 (2007).
[6] J. W. Belcher, L. Davis, and E. J. Smith, J. Geophys. Res. **74**, 2302 (1969).
[7] F. M. Neubauer *et al.*, Nature (London) **321**, 352 (1986).
[8] D. A. Roberts, M. L. Goldstein, and L. W. Klein, J. Geophys. Res. **95**, 4203 (1990).
[9] D. A. Gurnett *et al.*, J. Geophys. Res. **84**, 2029 (1979).
[10] P. J. Kellog *et al.*, Astrophys. J. **645**, 704 (2006).
[11] S. D. Bale *et al.*, Phys. Rev. Lett. **94**, 215002 (2005).
[12] E. Marsch *et al.*, J. Geophys. Res. **87**, 52 (1982).
[13] B. E. Goldstein *et al.*, Geophys. Res. Lett. **27**, 53 (2000).
[14] C.-Y. Tu, E. Marsch, and Z.-R. Qin, J. Geophys. Res. **109**, A05101 (2004).
[15] R. von Steiger *et al.*, Space Sci. Rev. **72**, 71 (1995).
[16] D. B. Reisenfeld *et al.*, J. Geophys. Res. **106**, 5693 (2001).
[17] J. A. Araneda, E. Marsch, and A.-F. Viñas, Phys. Rev. Lett. **100**, 125003 (2008).
[18] F. Valentini *et al.*, Phys. Rev. Lett. **101**, 025006 (2008).
[19] B. U. Ö. Sonnerup and S. Y. Su, Phys. Fluids **10**, 462 (1967).
[20] B. De Pontieu *et al.*, Science **318**, 1574 (2007).
[21] B. D. G. Chandran, Phys. Rev. Lett. **101**, 235004 (2008).
[22] P. H. Yoon and Ta-Ming Fang, Plasma Phys. Controlled Fusion **50**, 085007 (2008).
[23] J. C. Kasper, A. J. Lazarus, and S. P. Gary, Phys. Rev. Lett. **101**, 261103 (2008).
[24] G. G. Howes *et al.*, Phys. Rev. Lett. **100**, 065004 (2008).
[25] S. A. Markovskii *et al.*, Astrophys. J. **675**, 1576 (2008).
[26] K. Kauffmann and J. A. Araneda, Phys. Plasmas **15**, 062106 (2008).
[27] C. B. Wang, C. S. Wu, and P. H. Yoon, Phys. Rev. Lett. **96**, 125001 (2006).
[28] C. S. Wu and P. H. Yoon, Phys. Rev. Lett. **99**, 075001 (2007).
[29] D. H. Froula, L. Divol, and S. H. Glenzer, Phys. Rev. Lett. **88**, 105003 (2002).
[30] S. P. Gary and S. Saito, J. Geophys. Res. **108**, 1194 (2003).
[31] M. Heuer and E. Marsch, J. Geophys. Res. **112**, A03102 (2007).
[32] E. Marsch *et al.*, J. Geophys. Res. **87**, 35 (1982).
[33] H. F. Astudillo *et al.*, J. Geophys. Res. **101**, 24423 (1996).